HOW THE EUROPEAN CYCLONE TRACKS AND FREQUENCY CHANGED IN THE 1957-2002 PERIOD?

R. Pongrácz[1], J. Bartholy[1], M. Pattantyús-Ábrahám[2] and ZS. Pátkai[1]

[1]Department of Meteorology, Eötvös Loránd University, Budapest, Hungary, prita@nimbus.elte.hu, bari@ludens.elte.hu, a2zsolt@freemail.hu
[2]Department of Hydraulic and Water Resources Engineering, Budapest University of Technology and Economics, Budapest, Hungary, patyi@nimbus.elte.hu

Abstract. Variability and trend of the large-scale circulation characteristics over the North-Atlantic-European region are analyzed for the 20th century. First, changes in decadal frequency of Hess-Brezowsky macrocirculation patterns (MCP) are evaluated between 1881 and 2000. Then, cyclone center identification and cyclone tracks and intensity analysis is accomplished on the base of the European Centre for Medium-range Weather Forecast (ECMWF) reanalysis datasets (ERA-40) on a 2.5° horizontal resolution grid for the 45 year period between 1957 and 2002. Time series of the four main geopotential height fields (i.e., AT 500 hPa, AT 700 hPa, AT 850 hPa, and AT 1000 hPa) are used together with the sea level pressure fields. Decadal scale variability and trends are analyzed and compared for all levels. Finally, significant frontal events (e.g., frontal precipitation and temperature changes) are also analyzed, i.e., how often and how intense they occurred in the last few decades, whether or not any trend may be detected in the Carpathian Basin.

Keywords. Cyclone track, cyclone intensity, Atlantic-European region, macrocirculation pattern

1. Introduction

Extratropical cyclones are responsible for a large portion of the heat and moisture transports between the tropics and the polar regions. Therefore, any changes in frequency or intensity of these cyclones may affect significantly the regional climate of the midlatitudes. Several methodological approaches are available and have been applied to these analyses. One of the most often used statistical methods is to analyze the frequency change of macrocirculation patterns (MCP) defined for Europe by Hess and Brezowsky (1977) or defined for the region of the British Isles by Lamb (1972). Another method can also be used, namely, to extract and analyze the extratropical cyclones and their tracks since midlatitude cyclones are important features of the extratropical climate. In earlier studies midlatitude cyclones were subjectively identified by van Bebber (1891) and Klein (1957). Then, objective identification was used by Lambert (1988) and Hodges (1994). Zhang et al. (2004) composed the climatology of cyclone activity in the arctic regions for the 1948-2002, while Alpert et al. (1990) analyzed monthly cyclone frequencies and cyclone tracks based on 5-year-long (1982-1987) seven geopotential level fields for the Mediterranean region. Both analyses used data with 2.5° horizontal resolution. Key and Chan (1999) analyzed seasonal and annual trends of cyclone frequencies using time series of 1000 hPa and 500 hPa geopotential fields for 1958-1997 (with a latitude-longitude grid resolution of 2.5°×5°). Statistically significant increasing trends (at 0.05 level) were found in all seasons at 1000 hPa for the Arctic region.

In this paper, first, significant changes in the frequency of different Western/Central-European macrocirculation patterns are presented for the 20th century (Section 2). Then, in Section 3 cyclone tracks and intensity analysis is accomplished for the North-Atlantic-European region on the base of the European Centre for Medium-range Weather Forecast (ECMWF) reanalysis datasets (ERA-40) with 2.5° horizontal resolution. Changes of frontal activity in the Carpathian Basin are also analyzed.

2. Observed tendency of frequency of macrocirculation patterns

Phenomenological circulation statistics are analyzed using the Hess-Brezowsky (1977) macrocirculation types. Overview of the regional circulation structures of the Atlantic-European region can be found in Table 1. The macrocirculation patterns are classified into 29 types based on the

dominant direction of air mass movements and the presence of cyclones or anticyclones in different regions. The available dataset consists of daily MCP codes from 1881 to 2000 and is published monthly in the journal "Die Grosswetterlagen Europas" of the German Meteorological Service.

Table 1. Macrocirculation types defined in the Hess-Brezowsky classification system.

Circulation type	Main flow direction	Macrosynoptic type (notation)
Zonal	West (W)	West anticyclonic (Wa)
		West cyclonic (Wz)
		Southern West (Ws)
		Angleformed West (Ww)
Half-Meridional	Southwest (SW)	Southwest anticyclonic (SWa)
		Southwest cyclonic (SWz)
	Northwest (NW)	Northwest anticyclonic (NWa)
		Northwest cyclonic (NWz)
	Central European high (HM)	Central European high (HM)
		Central European ridge (BM)
	Central European low (TM)	Central European low (TM)
Meridional	North (N)	North anticyclonic (Na)
		North cyclonic (Nz)
		North, Iceland high, anticyclonic (HNa)
		North, Iceland high, cyclonic (HNz)
		British Islands high (HB)
		Central European Trough (TRM)
	Northeast (NE)	Northeast anticyclonic (NEa)
		Northeast cyclonic (NEz)
	East (E)	Fennoscandian high, anticyclonic (HFa)
		Fennoscandian high, cyclonic (HFz)
		Norwegian Sea – Fennoscandian high, anticyclonic (HNFa)
		Norwegian Sea – Fennoscandian high, cyclonic (HNFz)
	Southeast (SE)	Southeast anticyclonic (SEa)
		Southeast cyclonic (SEz)
	South (S)	South anticyclonic (Sa)
		South cyclonic (Sz)
		British Islands low (TB)
		Western European Trough (TRW)

Figure 1 presents the decadal frequency distribution of Hess-Brezowsky MCP types using Box-Whisker plot diagrams, and the significance of the detected trends. Large differences between the upper and the lower quartile values (appearing as large boxes in the figure) may indicate considerable changes in frequency of the given MCP type during the 120 years. Furthermore, the entire range between the maximum and minimum values of the decadal frequency also highlights the variability of MCP type frequency. Below the x-axis, sign of the detected trends is presented, and the significant trend signs are shaded by grey. According to the results, frequency of several MCP types changed significantly.

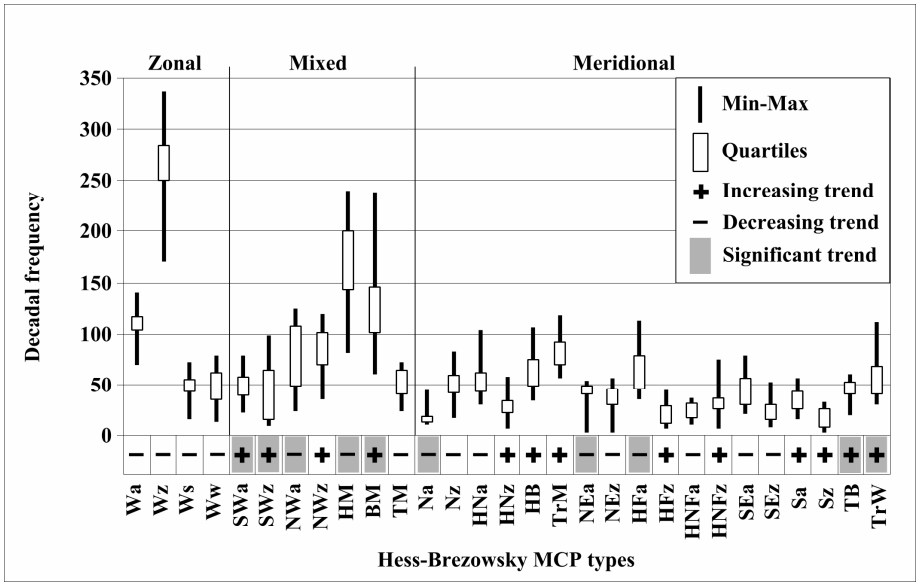

Figure 1. Decadal frequency distribution of Hess-Brezowsky types, 1881-2000. The description of the MCP types are listed in Table 1.

Figures 2 and 3 illustrate the increasing and decreasing tendency of occurrences, respectively. Frequencies of Southwest cyclonic (SWz), Central European ridge (BM), and Western European Trough (TrW) MCP types increased considerably during the 20th century. Frequencies of Northwest anticyclonic (NWa), Central European high (HM), and Fennoscandian high, anticyclonic (HFa) MCP types decreased in the last 120 years, all of them represent anticyclonically dominated circulation features over the European continent. At the lower panels of the figures, the typical sea level pressure patterns of the corresponding MCP types are provided.

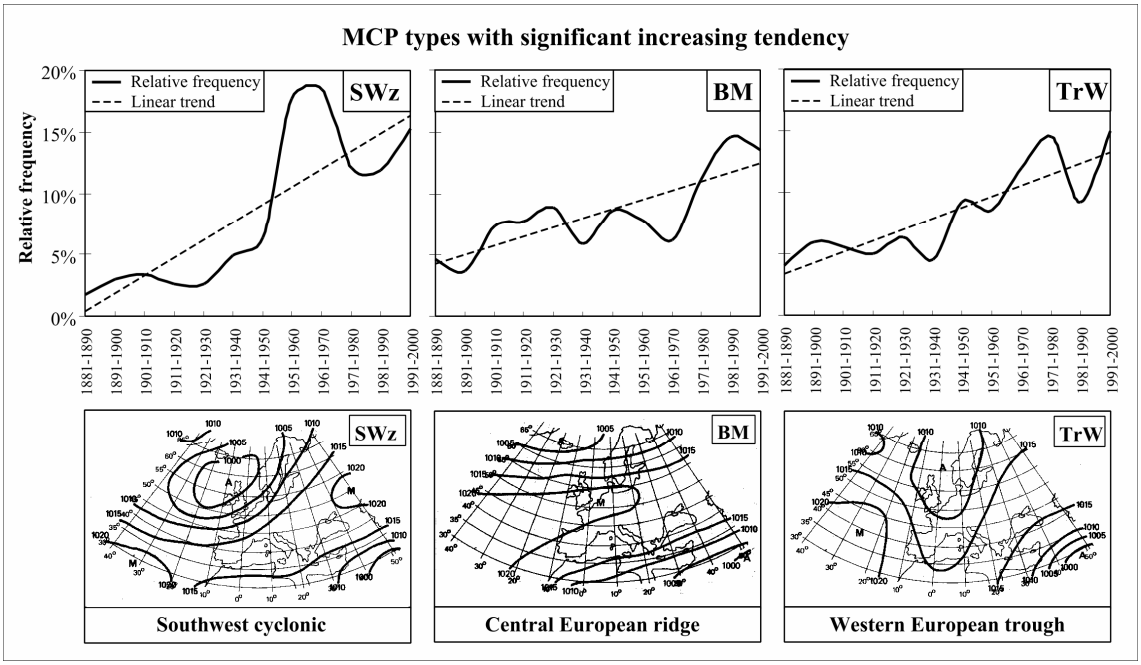

Figure 2. Selected Hess-Brezowsky MCP types with increasing decadal frequency distribution (1881-2000). The linear trend is fitted using the least square method. The description of these MCP types are listed in Table 1. Maps represent the typical sea level pressure patterns.

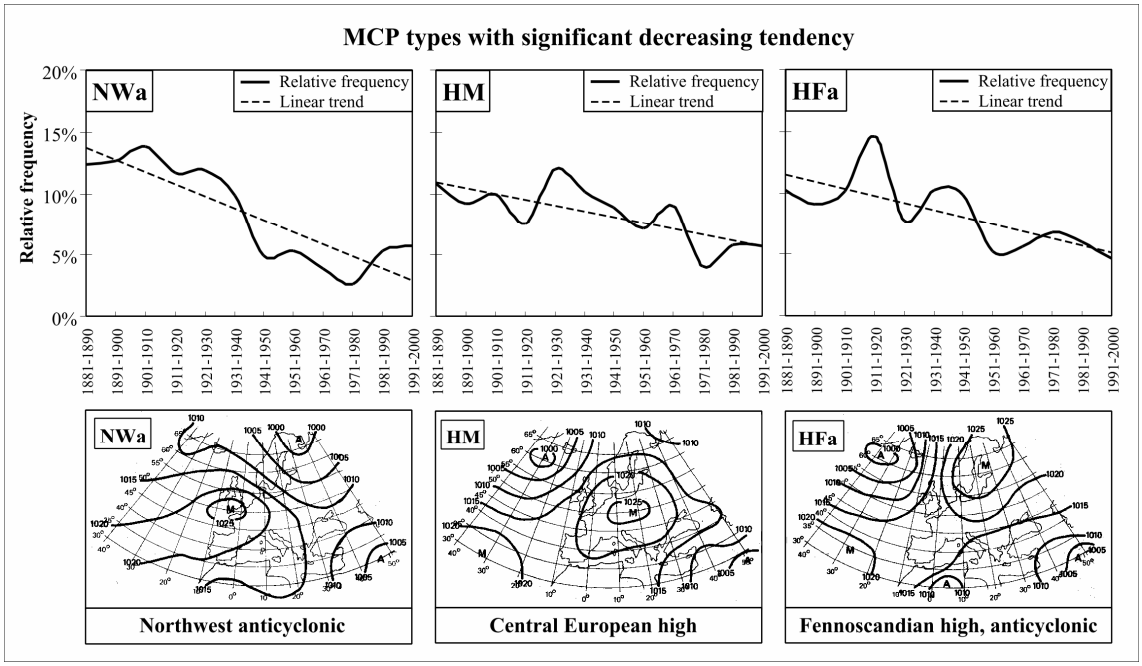

Figure 3. Selected Hess-Brezowsky MCP types with decreasing decadal frequency distribution (1881-2000). The linear trend is fitted using the least square method. The description of these MCP types are listed in Table 1. Maps represent the typical sea level pressure patterns.

Since these Hess-Brezowsky MCP types, as well, as the classification method include many subjective elements, the results presented in this section also involve a lot of uncertainty. In order to reduce this, objective algorithms are used in the next section for cyclone track identification.

3. Identification and analysis of European cyclone tracks

In the Northern hemisphere, midlatitude cyclones with their associated frontal systems influence significantly the local weather in Europe, as well as in most parts of North-America. For instance, more than two-thirds of the winter precipitation amount of the European continent originate from the frontal systems of less than 15 cyclones (Fraedrich et al., 1986), further highlighting the importance of cyclone track and cyclone intensity analysis.

3.1. Data

In the present analysis the European Centre for Medium-range Weather Forecast (ECMWF) reanalysis datasets (ERA-40) are used.

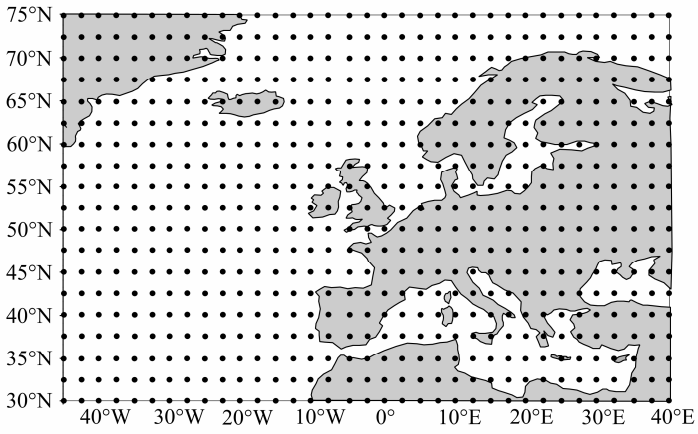

Figure 4. The selected domain and the grid points of the North-Atlantic-European region.

ERA-40 (http://www.ecmwf.int/research/era) has been compiled from both in-situ and remotely-sensed measurements made over the period since mid-1957 until 2002 (Kallberg et al., 2004). ERA-40 datasets provide all meteorological variables at 60 vertical levels between the surface and a height of about 65 km with 6-hour temporal resolution. Originally, ERA-40 has a spectral representation based on a triangular truncation at wave number 156 or 1.125° horizontal resolution using a Gaussian grid (Simmons and Gibson, 2000). The spatial resolution of the four main geopotential height fields (or Absolute Topography - AT) used in this analysis (i.e., AT 500 hPa, AT 700 hPa, AT 850 hPa, and AT 1000 hPa) is 2.5°×2.5°, which can be downloaded via Internet. In this paper, the North-Atlantic-European region is shown in Figure 4. This entire domain covers the area between 30°-75°N and 45°W-40°E, and it consists of 665 (=19×35) grid points altogether.

3.2. Results and discussion

In order to explore the structural changes in geopotential height fields, statistical descriptive parameters are analyzed for the last 45 years. Figure 5 presents the standard deviation of the four main geopotential height fields (AT-500 hPa, AT-700 hPa, AT-850 hPa, AT-1000 hPa) of the troposphere. Large standard deviation values indicate high variability of the geopotential height level. They can be observed in the northern part of the selected domain, namely, around Iceland. In general, the North-Atlantic-European region can be characterized by zonal distribution of standard deviation. Two disturbances can be identified, namely, (i) in the northwestern part of the selected domain where the large variance may partly be explained by frequent cyclogenesis, (ii) in the Ligurian/Tyrrhenian Sea with smaller standard deviation values where the so-called Genoa cyclones are often forming.

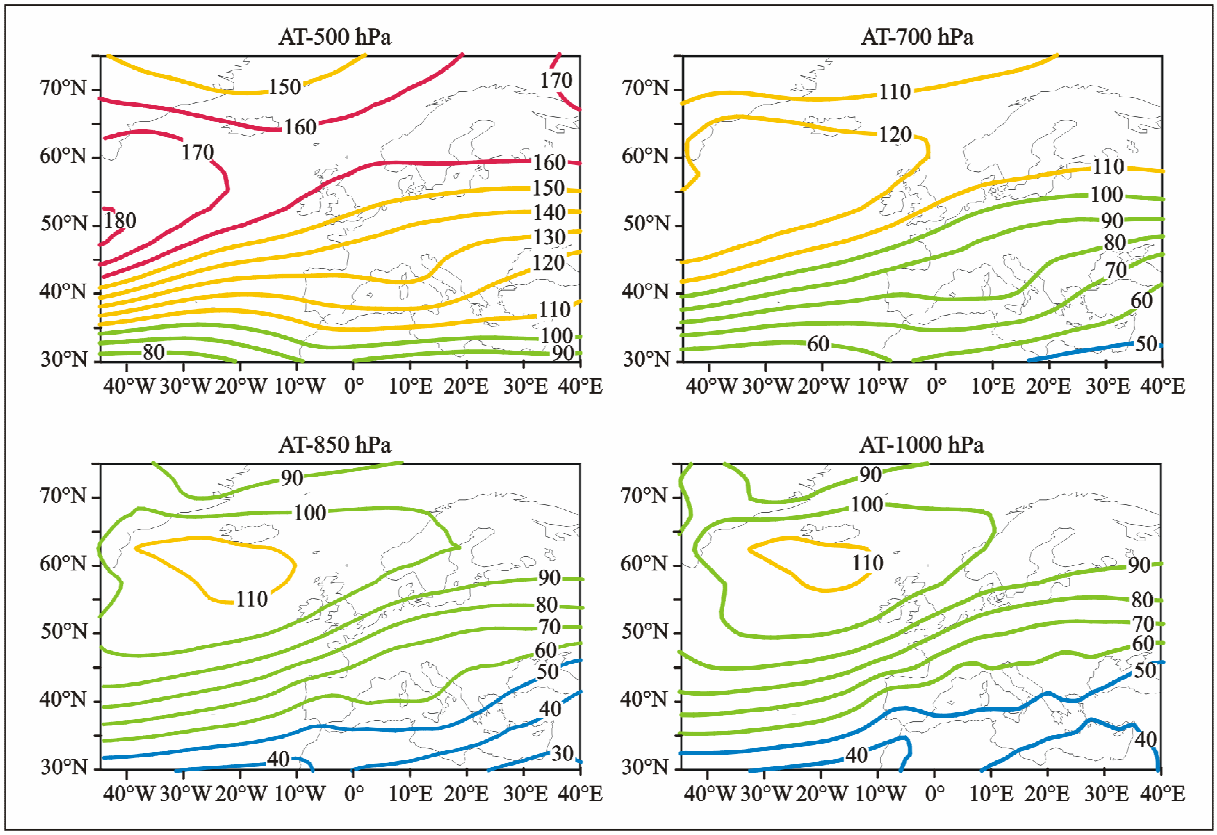

Figure 5. Standard deviation of the four main geopotential height fields for the North-Atlantic-European region, 1957-2002.

Linear tendency analysis is accomplished for all the grid points of the North-Atlantic-European domain. Decadal trend values are presented on the maps of Figures 6 and 7 for the middle and the lower tropospheric levels, respectively. Similar spatial structures can be seen on these maps representing different geopotential height levels. Special zonal patterns may be recognized with

negative trend coefficients with one center area in the Greenland/Iceland region, while positive trend coefficients dominate the southern area, where two centers can be identified: (1) in the Mediterranean and (2) in the Atlantic regions. On the maps, white and red asterisks represent the northern and the southern central regions, respectively. Graphs, shown above the maps of Figures 6 and 7, present the decreasing tendency of the annual mean geopotential height values for the grid point located in the Atlantic Ocean between southern Greenland and Iceland at 65°N latitude, 35°W longitude. Graphs, shown below the maps, illustrate the increasing tendency of the annual mean geopotential height values for the grid point located in the Mediterranean Sea at 42.5°N latitude, 7.5°E longitude. Except the AT 1000 hPa level, all of the presented linear trends for these two selected grid points are significant at 0.05 level using the t-test.

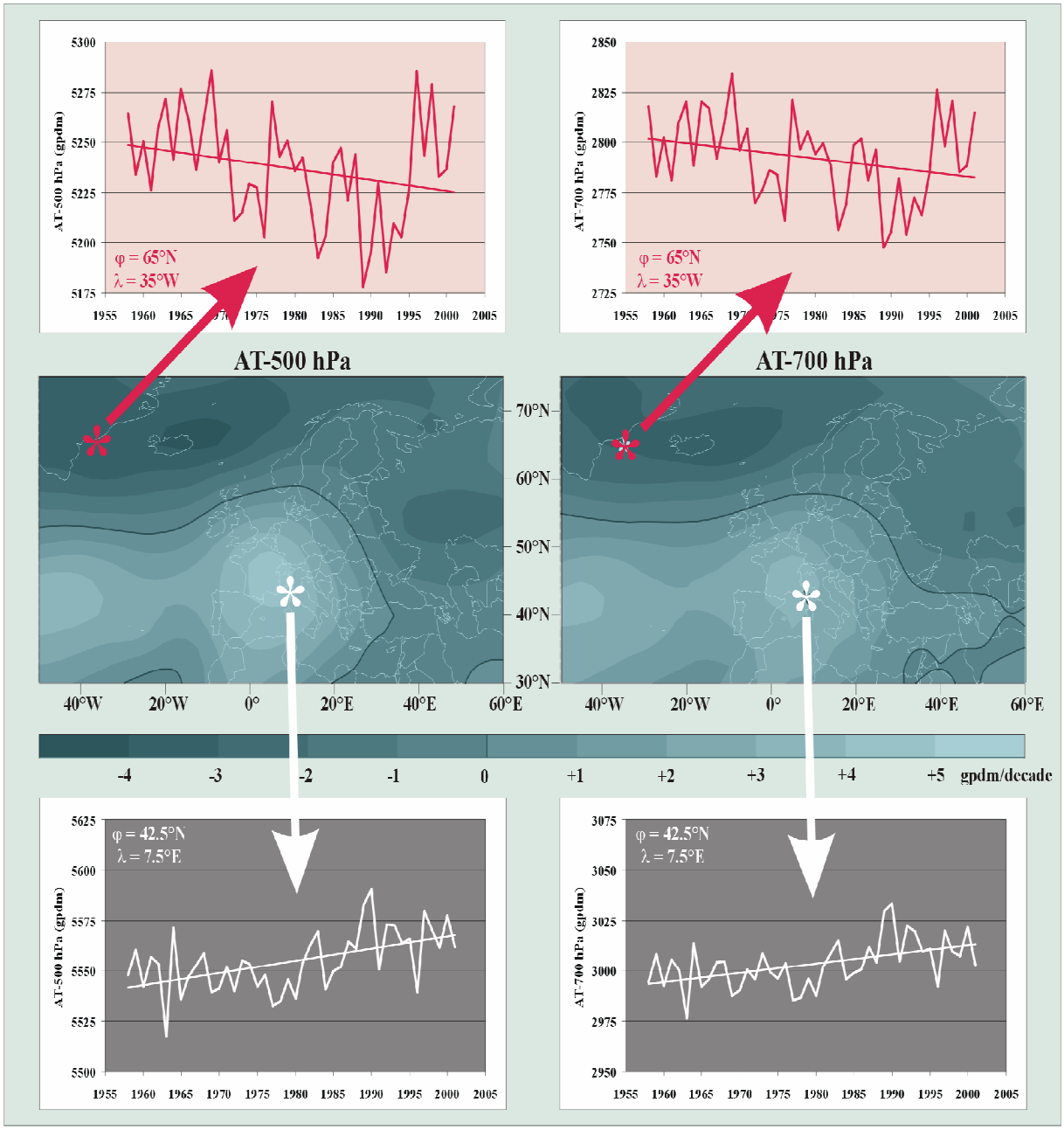

Figure 6. Tendency analysis of AT-500 hPa (left) and AT-700 hPa (right) geopotential height levels. Detailed linear trends are shown for two selected gridpoints (65°N 35°W and 42.5°N 7.5°E) above and below the map of the trend coefficients, respectively. The fitted linear trends are significant at 0.05 level using the t-test.

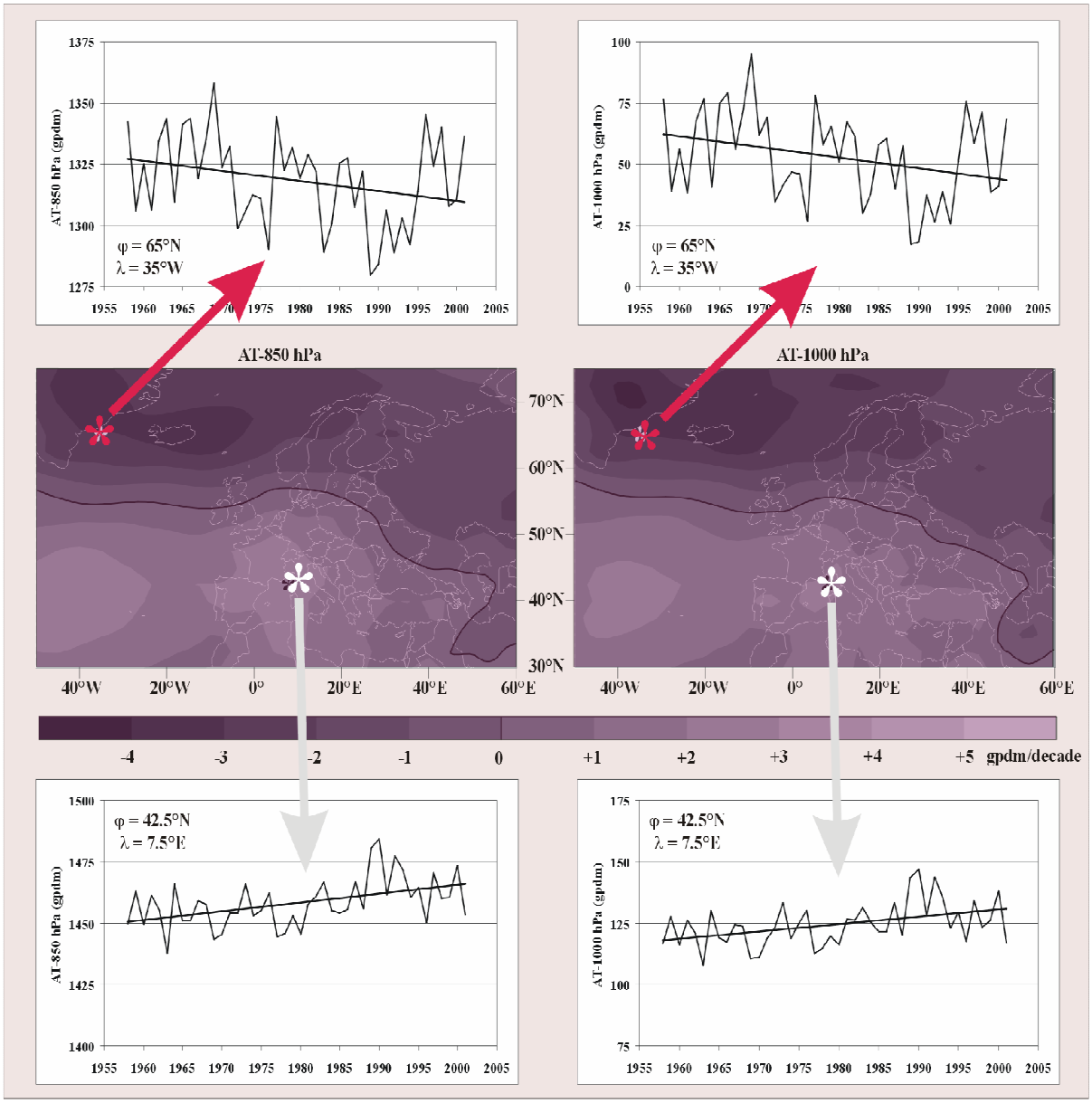

Figure 7. Tendency analysis of AT-850 hPa (left) and AT-1000 hPa (right) geopotential height levels. Detailed linear trends are shown for two selected gridpoints (65°N 35°W and 42.5°N 7.5°E) above and below the map of the trend coefficients, respectively. The fitted linear trends are significant at 0.05 level using the t-test only in case of AT-850 hPa.

After the evaluation of the annual trend maps, the seasonal trend coefficients are mapped for the four main geopotential height fields. Figure 8 presents the detected trend fields for the AT 500 hPa level. No significant trend can be found in summer (coefficients are below 1 gpm/decade in absolute value), while the largest trend coefficients are detected in winter. The structure of the winter trends is similar to the annual trend fields. However, the absolute values of the winter trend coefficients at the two centers (the northwestern part of the selected domain around Greenland/Iceland, and the Mediterranean region in southwestern Europe and the Ligurian/Tyrrhenian Sea) are larger than the annual trend coefficients.

One of the main advantages of compiled global reanalysis datasets is to open the possibility for the identification of cyclone centers and cyclone tracks using objective methodology. After obtaining the location of identified midlatitude cyclones, frequency and intensity analysis can be accomplished. Several authors attempted to identify extratropical cyclones using different algorithms but probably the most often cited method was developed by Serreze (1995) and Serreze et al. (1997). They studied

arctic cyclones occurring in spring and winter, 1973-1992, based on sea level pressure data with 2.5° horizontal resolution. Their results suggest that frequency of cyclones increased, while their lifetime decreased. The method applied by Serreze et al. (1997) derives cyclones using pressure gradient, and is able to detect strong high-latitude cyclones.

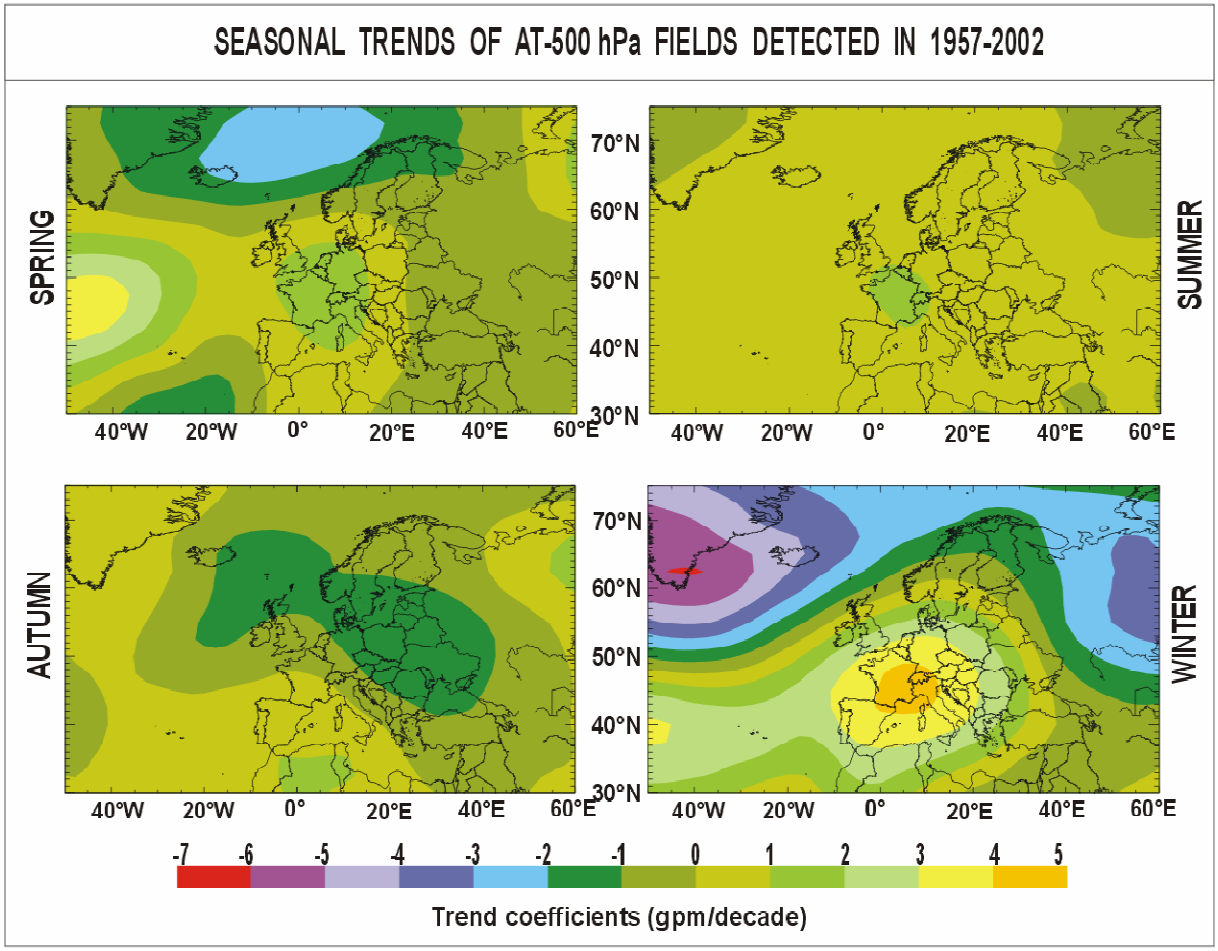

Figure 8. Seasonal trend analysis of AT-500 hPa geopotential height level, 1957-2002.

In this paper potential midlatitude cyclone centers are defined on grid points with pressure depression where the following main criteria are fulfilled: (1) the sea level pressure is less than 1012 hPa, and (2) the pressure gradient is greater than 0.07 hPa/100 km for all direction. Geographical latitude and longitude, sea level pressure, and minimum of the pressure gradient values of the potential cyclone centers are stored at every time step (i.e., 6 hours).

Then, cyclone tracks are determined by special sequences of stored potential cyclone centers. According to the algorithm used in this paper, two subsequent potential cyclone centers may belong to the same cyclone track if (1) their geographical distance is less than 900 km, and (2) their sea level pressure difference is less than 5 hPa in absolute value. Finally, the stored cyclone tracks contain data on (i) the time of the first detection of the cyclone center, (ii) the number of time steps until the last detection, (iii) the minimum pressure gradient during the entire lifetime of the cyclone, (iv) the geographical latitude/longitude coordinates of the cyclone center and (v) the sea level pressure in each time step. In order to verify the obtained cyclone tracks, synoptic charts of the North-Atlantic-European region have been used for June 2002 (one example is shown in Figure 9). Although slight shifts (a few degrees) in the location of cyclone centers occurred, no false cyclone track has been determined during the verification period.

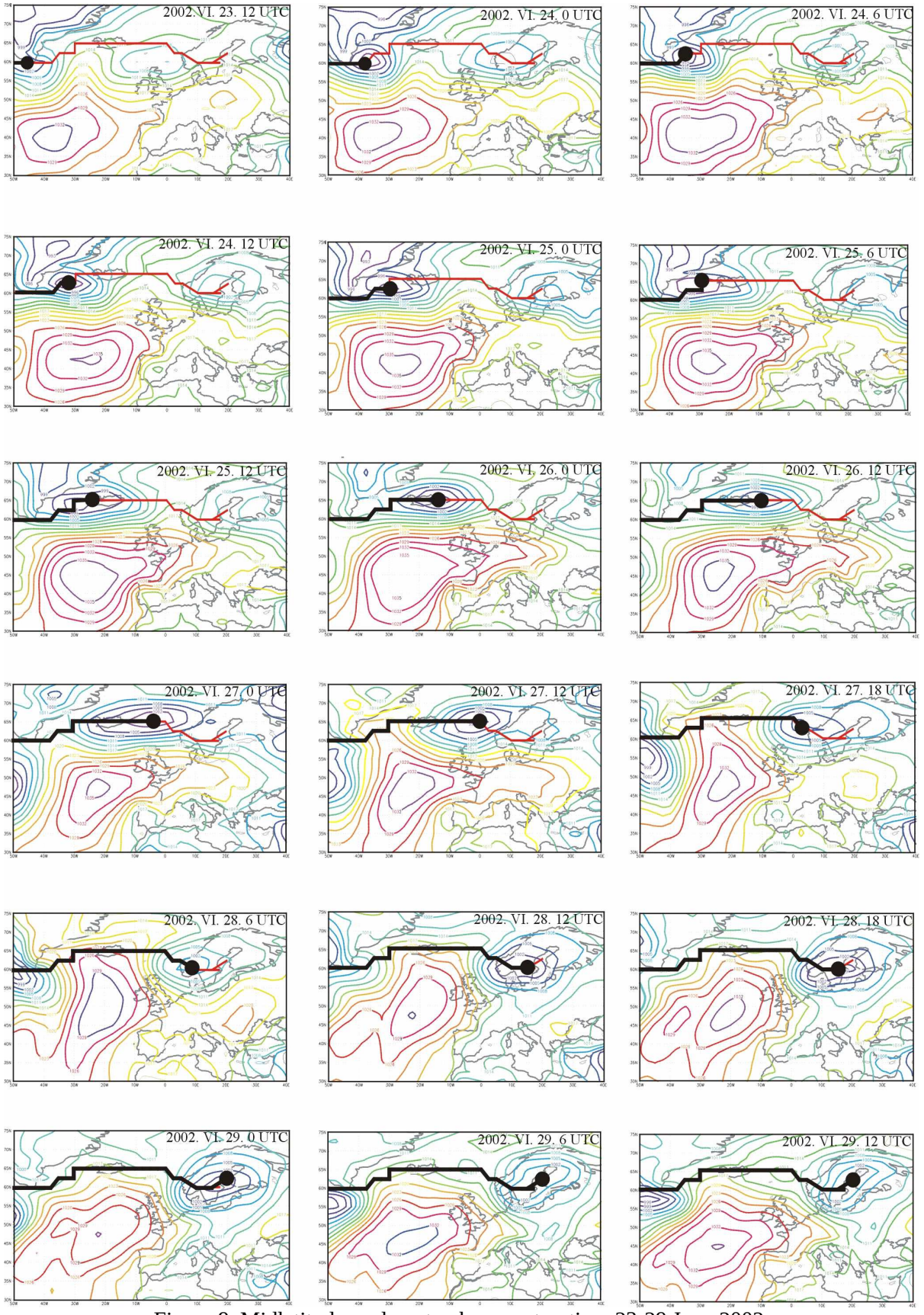

Figure 9. Midlatitude cyclone track reconstruction, 23-29 June 2002.

The starting positions of the identified midlatitude cyclone tracks indicate the geographical locations of cyclogenesis. Figure 10 shows the spatial frequency distribution of these cyclogenesis centers for the entire 45 years (1957-2002). The two largest frequency values can be found in the northwestern part of the selected domain around Greenland/Iceland, and in the Mediterranean region in southwestern Europe and the Ligurian/Tyrrhenian Sea – where the largest trend coefficients occurred (shown in Figures 6, 7, and 8).

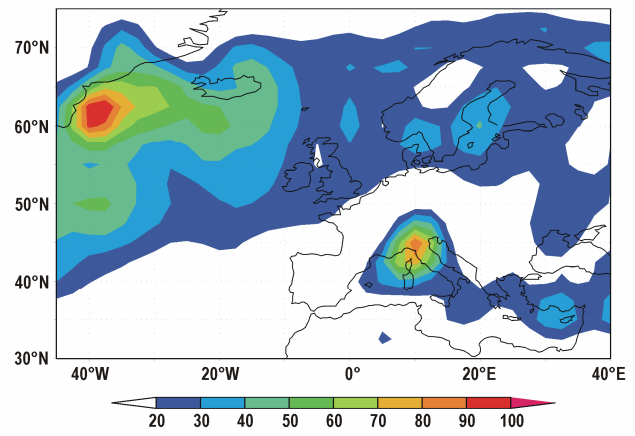

Figure 10. Frequency of cyclogenesis, 1957-2002.

Figure 11 summarizes seasonal cyclones center frequency in the North-Atlantic-European region for five equal 9-year-long periods. Maps on the left and the right panels represent smoothed grid point values in winter and summer, respectively. In general, less midlatitude cyclones can be detected in summer than in winter. Furthermore, cyclone tracks shift to the North in summer since they are located mainly north to the 50-55°N latitude zone. The results also suggest that the number of cyclones increased considerably in the northwestern part of the domain in the last 45 year in both seasons (Bartholy et al., 2006).

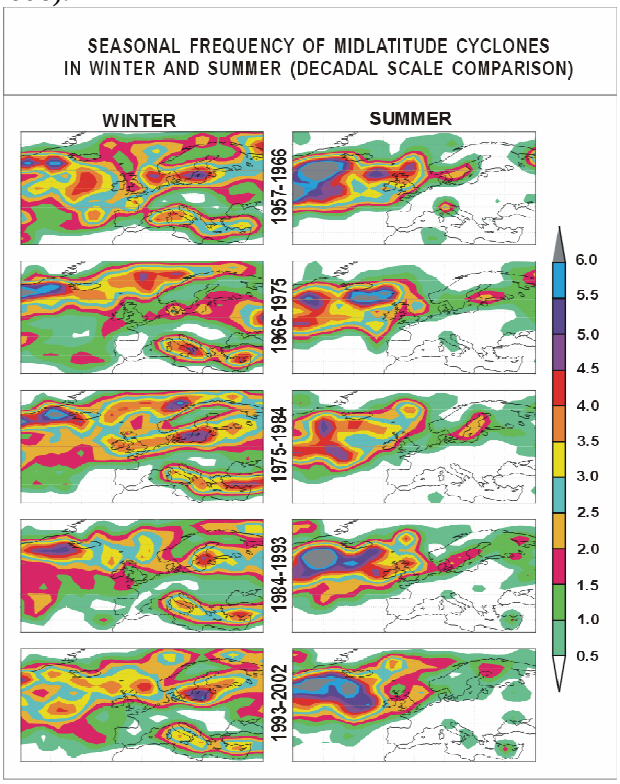

Figure 11. Changes of seasonal cyclone center frequency (per decade) distribution in the North-Atlantic-European region in winter (December-January-February) and summer (June-July-August).

In order to characterize the intensity of midlatitude cyclones, a complex parameter, namely, the Cyclone Activity Index (CAI) was defined by Zhang et al. (2004), which summarizes the differences between the sea level pressure of cyclone centers and the monthly mean pressure of that grid point for each time step of all cyclones detected in a given month. For the North-Atlantic-European region, seasonal CAI values are mapped in Figure 12. In order to detect the possible changes in cyclone activity, the entire 45-year-long period is separated into five equal long subsets similarly to the previous analysis. In general, the Icelandic cyclogenesis region is the most intense activity center on the maps. Genoa cyclone area is much weaker than the Icelandic low. Furthermore, winter cyclone activity is larger than CAI values in summer. The results suggest that a considerable intensification can be detected in cyclone activity in winter, especially, in the northwestern part of the domain. Further analysis of selected subregions would require different CAI-scale and dataset with finer spatial resolution.

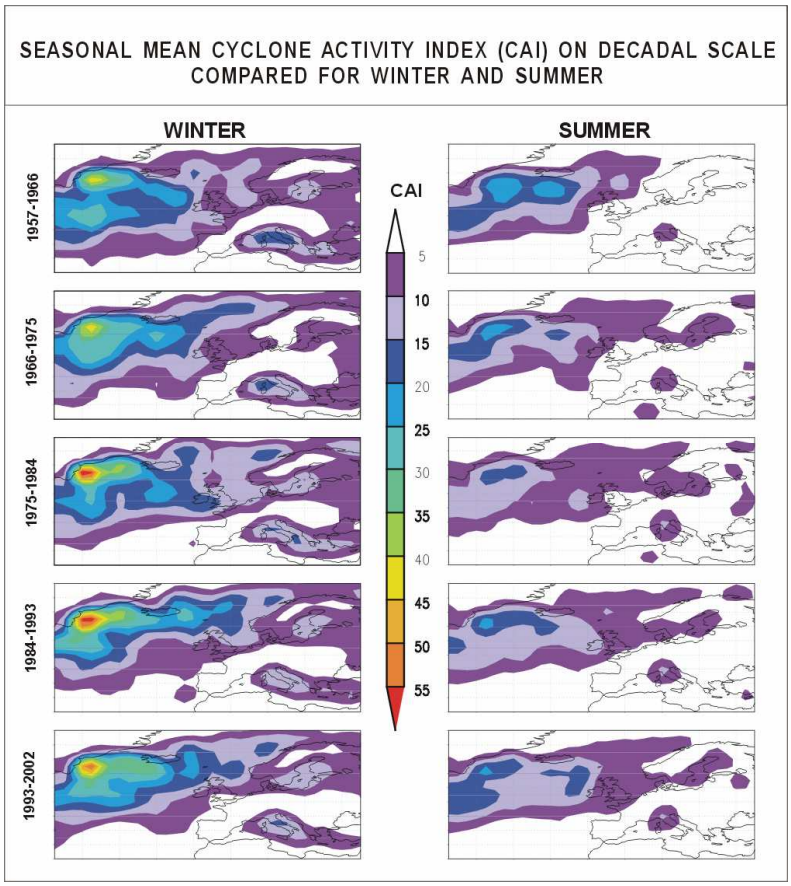

Figure 12. Changes of seasonal CAI values in the North-Atlantic-European region in winter (December-January-February) and summer (June-July-August).

As part of the cyclone activity, frontal systems are investigated in the last part of the paper. We are focusing on the cold and warm fronts passing over the Carpathian Basin. In our analysis, fronts are defined using the temperature values of 850 hPa geopotential height of the ERA-40 database (Kallberg et al., 2004). On the base of the synoptic practical guides, we assume that if the temperature change during 12 hours is more than 3°C it can be considered as a front by definition. Figure 13 presents the frequency distribution of the frontal systems. The total number of cold and warm fronts during the entire 45 year period is 2202 (58%) and 1580 (42%), respectively. According to the results, not only the number of the cold fronts occurred in the region is larger than the number of warm fronts, but the corresponding temperature change is also significantly larger in case of the cold fronts.

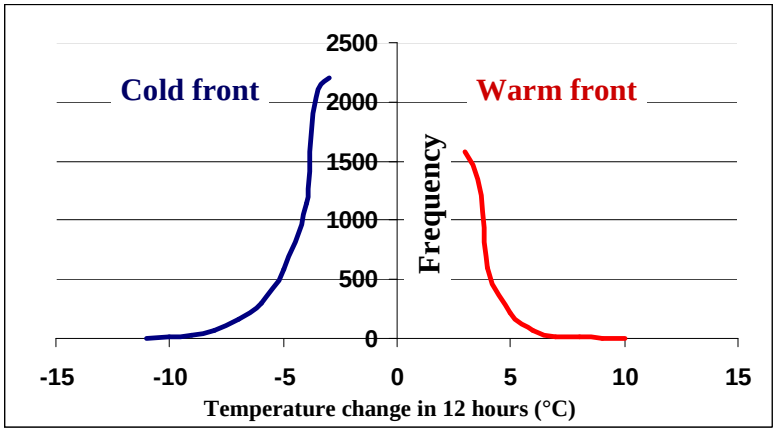

Figure 13. Frequency distribution of temperature changes in case of cold and warm frontal systems, 1957-2002.

Annual, seasonal, and monthly trends of the number of cold and warm fronts are determined. Figure 14 shows the annual tendency analysis of the cold and warm frontal systems in the upper and the lower panel, respectively. Four-year moving average (MA) and the fitted linear trend using the least squares method are presented in the graphs. The annual number of cold fronts increased more than the warm fronts between 1957 and 2002. The linear trend coefficients significantly differ from zero using the statistical t-test at 0.05 level of significance. Seasonal trend analysis is illustrated in Figure 15, where the significant positive tendencies of the cold fronts in autumn and the warm fronts in winter are presented.

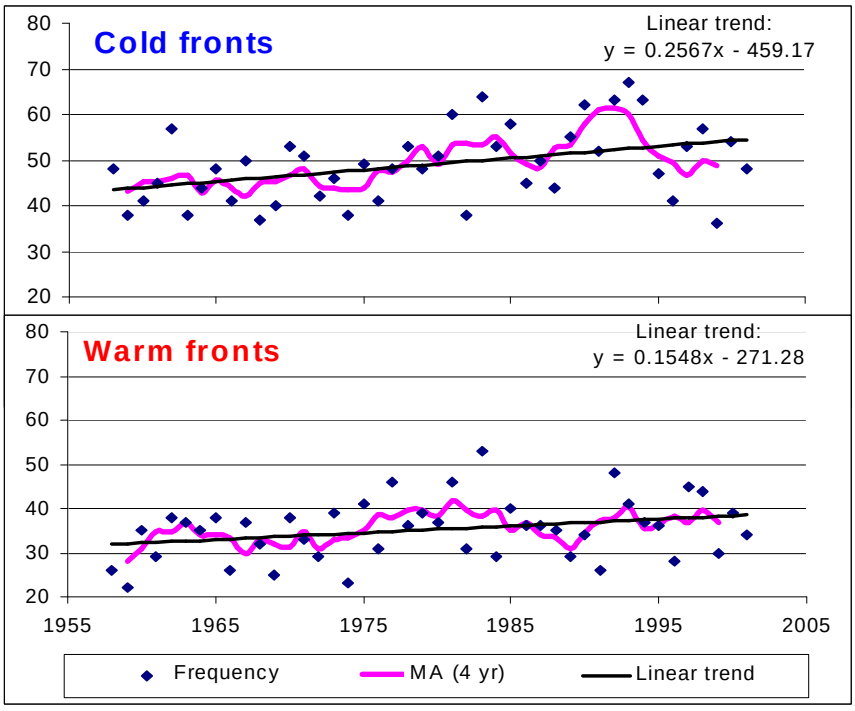

Figure 14. Annual tendency of cold and warm fronts (using criterion $\Delta T>3°C$), 1957-2002. Linear trend coefficients are significant at 0.05 level.

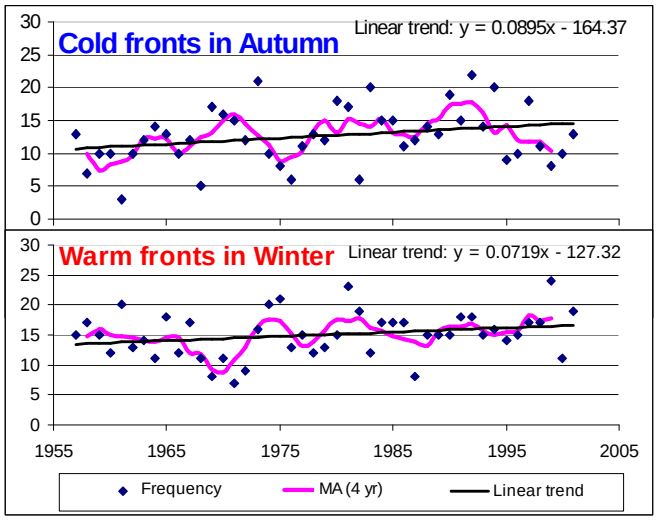

Figure 15. Seasonal tendency of cold fronts (in autumn) and warm fronts (in winter) using criterion ΔT>3°C, 1957-2002. Linear trend coefficients are significant at 0.05 level.

Precipitation events associated with the frontal systems strongly affect the regional climate, therefore, at the end of the paper we present the results of the frontal precipitation analysis. Several thresholds (i.e., 0 mm, 1 mm, 5 mm, 10 mm) are defined, and then, the annual and the seasonal numbers of cold and warm frontal precipitation events exceeding these thresholds are determined during the 1957-2002 period. Figures 16 and 17 present the annual trend analysis of the cold and warm frontal precipitation events, respectively. Annual number of cold frontal precipitation events increased in the last 45 years (the positive trend is significant in case of 0 mm, 1 mm, 5 mm thresholds at 0.05 level). The largest seasonal trend coefficients can be detected in spring and autumn. Annual number of warm frontal precipitation events decreased between 1957 and 2002 (the negative trend is significant in case of 1 mm, 5 mm, 10 mm thresholds at 0.05 level). The largest seasonal trend coefficients (in absolute value) can be detected in winter.

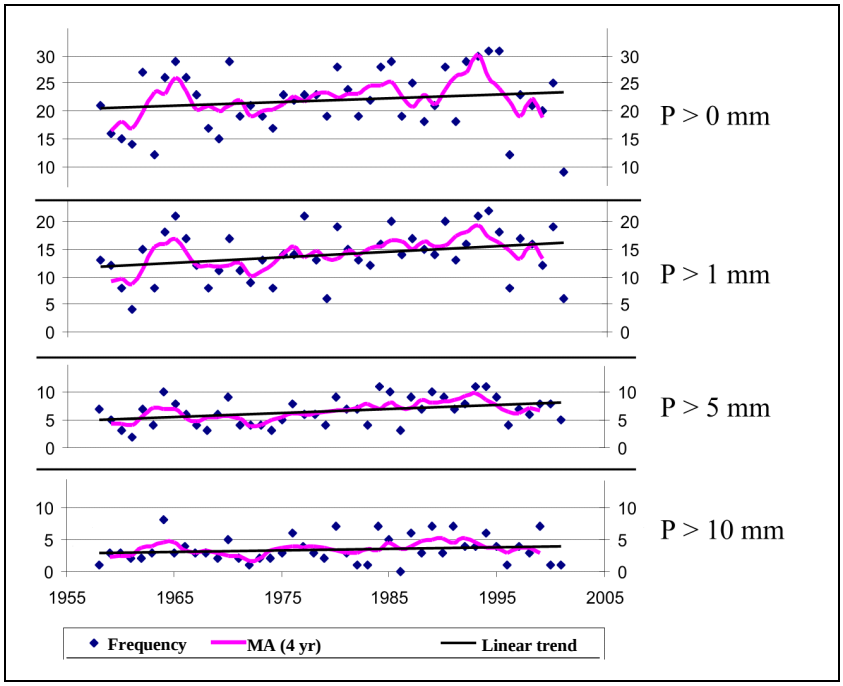

Figure 16. Annual tendency of cold frontal precipitation using criterion ΔT>3°C, 1957-2002. Linear trend coefficients are significant at 0.05 level except using the 10 mm threshold.

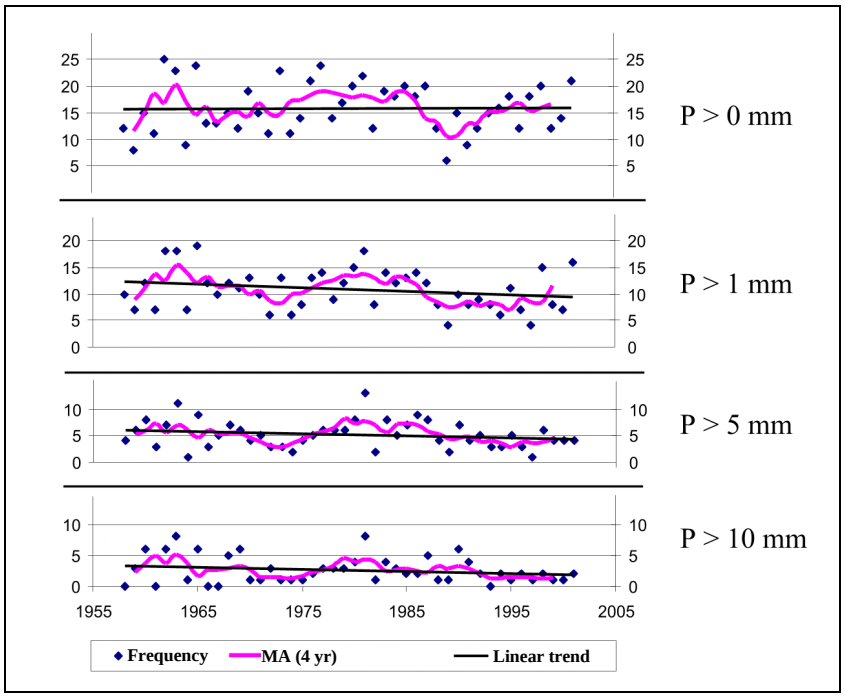

Figure 17. Annual tendency of warm frontal precipitation using criterion ΔT>3°C, 1957-2002. Linear trend coefficients are significant at 0.05 level except using the 0 mm threshold.

4. Conclusions

Changes in large-scale circulation have been analyzed for the North-Atlantic-European region for the 20th century. In order to accomplish this task, time series of MCP types (1881-2000) and height fields of four geopotential levels of the ERA-40 database (1958-2002, with 2.5° horizontal resolution) have been used. Based on the presented results, the following conclusions can be drawn.

1. Frequency of many anticyclonic Hess-Brezowsky MCP types has decreased significantly in the last 120 years. Several other Hess-Brezowsky MCP types performed considerable increase between 1881 and 2000.

2. Decreasing tendency of the annual mean geopotential height values has been detected in the Greenland/Iceland region between 1957 and 2002, while positive trend coefficients dominate the southern area of the North-Atlantic-European region with two centers, one in the Mediterranean subregion and the other in the Atlantic subregion. The largest seasonal trends can be detected in case of winter with similar spatial structure.

3. Less midlatitude cyclones occurred and cyclone tracks shifted more to the North in summer than in winter in the last 45 years. Furthermore, the number of cyclones increased considerably in the northwestern part of the domain in both seasons.

4. The Icelandic cyclogenesis region is the most intense cyclone activity center in the North-Atlantic-European region. Furthermore, considerable intensification has been detected in cyclone activity between 1957 and 2002. CAI values in winter are larger than in summer.

5. Annual number of both cold and warm frontal systems in the Carpathian Basin increased significantly during the 1957-2002 period.

6. Cold frontal precipitation events increased in the region during the 45 years, especially in spring and autumn, while warm frontal precipitation events decreased, especially in winter.

Acknowledgements. The authors thank ECMWF for producing and making available the ERA-40 reanalysis data. This paper is the written version of the presentation at the special session of ECAM-2005 conference organized in the frame of COST Action 733. Research leading to this paper has been supported by the Hungarian National Science Research Foundation under grants T-034867, T-038423, and T-049824, also by the CHIOTTO project of the European Union Nr. 5 program under grant

EVK2-CT-2002/0163, and the Hungarian National Research Development Program under grants NKFP-3A/0006/2002, NKFP-3A/082/2004, and NKFP-6/079/2005.

References

Alpert P, Neeman BU, Shay-el Y. 1990. Climatological analysis of Mediterranean cyclones using ECMWF data. Tellus 42A: 65-77.

Bartholy, J., Pongrácz, R., Pattantyús-Ábrahám, M. 2006. European cyclone track analysis based on four geopotential fields of ECMWF ERA-40 datasets. Int. J. Climatology (in press)

van Bebber WJ. 1891. Die Zugstrassen der barometrischen Minima nach den Bahnenkarten der Deutschen Seewarte für den Zeitraum von 1870-1890. Meteorol. Zeitschrift 8: 361-366.

Fraedrich K, Bach R, Naujokat G. 1986. Single station climatology of Central European fronts: number, time, and precipitation statistics. Contr. Atmos. Phys. 59: 54-65.

Gibson JK, Kallberg P, Uppala S, Nomura A, Hernandez A, Serrano A. 1997. ERA description. ECMWF Reanalysis Project Report Series No. 1., 77p.

Hess P, Brezowsky H. 1977. Katalog der Grosswetterlagen. Berichte Deutscher Wetterdienst Offenbach. 113 Bd 15.

Hodges KI. 1994. A general method for tracking analysis and its application to meteorological data. Mon. Wea. Rev. 122: 2573-2586.

IPCC, 2001: Climate Change 2001: The Scientific Basis. Contribution of Working Group I to the Third Assessment Report of the Intergovernmental Panel on Climate Change. (Houghton JT, Ding Y, Griggs DJ, Noguer M, van der Linden PJ, Dai X, Maskell K, Johnson CA, eds.) Cambridge University Press: Cambridge, U.K. and New York, NY, USA. 881pp.

Kallberg P, Simmons A, Uppala S, Fuentes M. 2004. The ERA-40 archive. ERA-40 Project Report Series No. 17.

Key JR, Chan ACK. 1999. Multidecadal global and regional trends in 1000 mb and 500 mb cyclone frequencies. Geophys. Res. Lett. 26: 2053-2056.

Klein W. 1957. Principal tracks and mean frequencies of cyclones and anticyclones in the Northern hemisphere. Research Paper No. 40. U.S. Weather Bureau: Washington.

Lamb HH. 1972. British Isles weather types and a register of the daily sequence of circulation patterns, 1861-1971. Geophys. Mem. 116. HMSO: London.

Lambert SJ. 1988. A cyclone climatology of the Canadian Climate Centre general circulation model. J. Climate 1: 109-115.

Serreze MC. 1995. Climatological aspects of cyclone development and decay in the Arctic. Atmosphere-Ocean 33: 1-23.

Serreze MC, Carse F, Barry R. 1997. Icelandic low cyclone activity: Climatological features, linkages with the NAO, and relationships with recent changes in the Northern Hemisphere circulation. J. Climate 10: 453-464.

Zhang X, Walsh JE, Zhang J, Bhatt US, Ikeda M. 2004. Climatology and interannual variability of arctic cyclone activity: 1948-2002. J Climate 17: 2300-2317.